ISSN 0915-633X

NATIONAL INSTITUTE FOR FUSION SCIENCE

Solitary Radial Electric Field Structure in Tokamak Plasmas

K. Itoh, S.-I. Itoh, M. Yagi and A. Fukuyama

(Received - Nov. 5, 1997)

NIFS-525 Dec. 1997

RESEARCH REPORT
NIFS Series

NAGOYA, JAPAN

Solitary Radial Electric Field Structure in Tokamak Plasmas

K. Itoh, S.-I. Itoh*, M. Yagi*, A. Fukuyama†

National Institute for Fusion Science, Nagoya 464-01, Japan
**Research Institute of Applied Mechanics, Kyushu University 87, Kasuga 816, Japan*
†Faculty of Engineering, Okayama University, Okayama 700, Japan

Abstract

The solitary structure solution of the radial electric field E_r in the tokamak plasmas is obtained. It is shown to be stable under the external power supply like a biased electrode. The radial gradient is governed by the ion viscosity and the nonlinearlity of the perpendicular conductivity. The radial structure of E_r and reduction of turbulent transport are self-consistently determined. A bifurcation from a radially-uniform one to solitary one occurs at a certain applied voltage, and a hysteresis is associated.

Keywords: radial electric field, shear viscosity, solitary structure, biased electrode, bifurcation, suppression of turbulence

The finding of the H-mode in tokamak plasmas [1] is one of the first experimental demonstration of the structural transition in confined plasmas, which are in the far-nonequilibrium state. The electric field bifurcation has been proposed for the mechanism of the H-mode transition [2], and the important role of the structure of the radial electric field E_r on the plasma confinement is now widely recognized (see review, e.g., [3,4].) Related with the electric field, the impact on the micro turbulence has been investigated most intensively. In this process, the radial inhomogeneity of E_r is considered to play a crucial role [5-7]. The interface between the plasmas with different electric polarity was discussed [8, 9]. Motivated by the H-mode physics, the experiment has been done by use of the biased electrode near the plasma periphery [10], to study the nonlinear dependence between the radial current and E_r and to control them. The data provides a basic information to understand the plasma nonlinearlity that induces the electric field bifurcation. Several attempts of analysis have been done [11], but the spatial structure of E_r is not fully understood. In particular, the physics mechanism that determines the gradient of E_r is left unresolved.

In this article, we study the spatial structure of the radial electric field in the presence of the radial current across the magnetic field. It is found that there exists a solution of solitary structure of E_r. The gradient and its impacts on the turbulence suppression are self-consistently determined. The ion viscosity, coupled with the nonlinearlity in the perpendicular conductivity, governs the gradient of the radial electric field. It is shown that the bifurcation of E_r takes place from a radially-homogeneous distribution to the solitary structure at a threshold voltage imposed on the electrode. Stability of this solitary structure is also discussed.

The radial electric field E_r is governed by the charge conservation relation combined with the Poisson's relation as $\frac{\partial}{\partial t}E_r = -\frac{1}{\varepsilon_0\varepsilon_\perp}\left(J_r^{NET} - J_{ext}\right)$ where J_r^{NET} is the net radial current in the plasma which flows across the magnetic surface, J_{ext} is the current which is driven into the electrode by the external circuit, ε_0 is the vacuum susceptibility, and $\varepsilon_\perp$ is a dielectric constant of the magnetized plasma. The radial current is composed of two components, $J_r^{NET} = J_r - \varepsilon_0\varepsilon_\perp \nabla \cdot \mu_i \nabla E_r$. The first term

J_r is the "local current", which is determined by the radial electric field at the same radial location. The second is caused by the shear viscosity of ions, μ_i, and includes the diffusion operator [3]. The equation of E_r is a nonlinear diffusion equation as

$$\frac{\partial}{\partial t}E_r = \nabla \cdot \mu_i \nabla E_r - \frac{1}{\varepsilon_0 \varepsilon_\perp}(J_r - J_{ext}) \,. \tag{1}$$

The local current J_r and E_r is related through the perpendicular conductivity

$$J_r = \sigma(E_r) E_r \,. \tag{2}$$

Many physics mechanisms influence on J_r, and the conductivity $\sigma(E_r)$ includes the nonlinear dependence on E_r. In this article, we study the case that the neoclassical current [11] is dominant in J_r. We are interested in the very steep gradient of E_r. Compared to the structure of E_r, the other plasma parameters are slowly varying in space, so that the other plasma parameters are treated constant for the simplicity. The pressure-driven radial current in the limit of $E_r = 0$ is neglected. However, this does not change the result qualitatively.

First, we study the case that the ion viscosity μ_i is constant. Effect of the electric field shear on μ_i is discussed later. The dependence of the conductivity on E_r is symbolically written as $\sigma(E_r) \equiv \sigma(0) f(X)$, where E_r is normalized as $X = e\rho_p E_r / T$ (ρ_p: ion poloidal gyroradius, T: ion temperature), and $f(X)$ satisfies the relations $f(0) = 1$ and $f(X) \to 0$ as $|X| \to \infty$. For the analytic treatment, we consider the radially-thin shell structure, and introduce the normalization in space and time as $x = (r - r_0)/\ell$ and $\tau = t / t_N$, where $\ell = \sqrt{\mu_i/\sigma(0)}$ and $t_N = \varepsilon_0 \varepsilon_\perp / \sigma(0)$. (The radius r_0 is chosen at the middle between two electrodes.) The current density is normalized as $I = (e\rho_p / T\sigma(0)) J_{ext}$. Then the basic equation for E_r is rewritten as

$$\frac{\partial}{\partial \tau}X = \frac{\partial^2}{\partial x^2} X - f(X)X + I \tag{3}$$

The solitary solution of electric field, which has cylindrical symmetry, is searched for. The solution is much localized than the distance between the two magnetic surfaces, on which the electrodes are located. The boundary condition is chosen as $\partial X/\partial x \to 0$ at $|x| \to \infty$. We choose $x = 0$ at the surface of the symmetry.

The perpendicular conductivity is calculated in the neoclassical theory [11]. In the collisionless limit, approximate form is given as $f(X) \simeq exp(-X^2)$. In a collisional case, the conductivity is modelled by the Lorentzian form as $f(X) \simeq 1/(\nu_*^2 + X^2)$.

The stationary solution is obtained. Schematic form of the local current $Xf(X)$ is illustrated in Fig.1. Equation (3) with $\partial/\partial\tau = 0$ has a trivial solution, which is constant in space, as

$$X = X_1 \tag{4}$$

where X_1 is the solution of the equation $f(X_1)X_1 = I$ (see Fig.1). Besides this trivial solution, there is a nontrivial solution with the solitary radial electric field. Equation (3) (with $\partial/\partial\tau = 0$) is multiplied by $\partial X/\partial x$ and is integrated as

$$\frac{1}{2}\left(\frac{dX}{dx}\right)^2 = \int_{X_1}^{X} Xf(X)dX - IX + const \equiv F(X) . \tag{5}$$

Qualitative feature of $F(X)$ is known from Fig.1. $F(X)$ takes the minimum at $X = X_1$ and the maximum at $X = X_2$, respectively. (X_1 and X_2 are the solutions of $Xf(X) = I$ as is shown in Fig.1) $F(X)$ is a decreasing function of X in the region of $X > X_2$. The constant of the integral is chosen as $F(X_1) = 0$. By this choice, the boundary condition at $|x| \to \infty$ is satisfied. The solution $X(x)$ is given as

$$x = \int^{X} \{2F(X)\}^{-1/2} dX . \tag{6}$$

This solution gives the solitary structure of the radial electric field.

The solution is studied near the critical current, $I \simeq I_*$, where the local current $Xf(X)$ takes the maximum with respect to X as is shown in Fig.1. Expanding $F(X)$ in Eq.(5) in the vicinity of $I \simeq I_*$, and keeping terms up to $(X - X_1)^3$ in $F(X)$, we have $F(X) = C\{(X_* - X_1)(X - X_1)^2 - (X - X_1)^3/3\} + \cdots$, and the solution is obtained as

$$X(x) = X_* + 3\alpha^2 - 3\alpha^2\left(\frac{e^{\alpha C x} - 1}{e^{\alpha C x} + 1}\right)^2 \tag{7}$$

where $\alpha \equiv C^{-1/4}(I_* - I)^{1/4}$ and $C = (-1/2)(\partial^2/\partial X^2)[Xf(X)]_{X = X_*}$. The peak height scales as $(I_* - I)^{1/2}$ and the width scales like $(I_* - I)^{-1/4}$.

To study the voltage-current relation quantitatively, let us take a model form $f(X) = 1 - X^2/3X_*^2$ ($|X| < \sqrt{3}X_*$) and $f(X) = 0$ ($|X| > \sqrt{3}X_*$). This model keeps an essential feature of the conductivity, i.e., f gradually becomes smaller if $|X|$ is small and $f << 1$ holds in the large $|X|$ limit. This form of f provides an exact analytic solution for the solitary radial electric field structure. For the parameter range of $X_*/\sqrt{3} < X_1 < X_*$, we have the solution as

$$X(x) = X_1 + \frac{2\sqrt{6}y_1^2}{\sqrt{1 - X_1^2/3X_*^2}}\left(exp(y_1 x) + exp(-y_1 x) + \frac{2\sqrt{2}X_1}{\sqrt{3X_*^2 - X_1^2}}\right)^{-1} X_* \tag{8}$$

where $y_1 = \sqrt{1 - X_1^2 X_*^{-2}}$. In the weak current case, $X_1 < X_*/\sqrt{3}$, we have

$$\begin{aligned} X(x) &= C_m\frac{X_*^2}{I} + \sqrt{3}X_* - \frac{I}{2}x^2 && |x| < x_c \\ X(x) &= \frac{4\sqrt{3}C_2 exp(y_1(x - x_c))\,X_*}{\{C_2 exp(y_1(x - x_c)) + 2X_1 X_*^{-1} y_1^{-2}/\sqrt{3}\}^2 + 2y_1^{-2}} + X_1 , && x > x_c \end{aligned} \tag{9}$$

where $x_c \equiv \sqrt{2C_m}X_* I^{-1}$ and numerical constants C_m and C_2 are defined as
$C_m = (\sqrt{3}X_* - X_1)^2(X_*^2 - X_1^2)^{-1}(1 + X_1/\sqrt{3}X_*)(1 - \sqrt{3}X_1/X_*)/4$,
$C_2 = (c_2 + \sqrt{c_3})(1 - X_1/\sqrt{3}X_*)^{-1}$, $c_2 \equiv 2(1 + X_1/\sqrt{3}X_*)(1 - 2X_1/\sqrt{3}X_*)(1 - X_1^2 X_*^{-2})^{-1}$,
$c_3 \equiv 2(1 + X_1/\sqrt{3}X_*)(1 - \sqrt{3}X_1/X_*)(1 - X_1^2 X_*^{-2})^{-1}$. Figure 2 illustrates the solitary

solution in the case of $X_1/X_* = 0.6$. In the small I limit, it is shown from Eq.(9) that the peak height and the width scales as $X_*^2 I^{-1}$ and $X_* I^{-1}$, respectively.

By performing the integral $V = \int_{-d/2}^{d/2} X(x)dx$, the voltage difference between the electrodes is calculated. (d is a distance between the electrode.) In the asymptotic limit $y_1 d >> 1$, one has explicit relations

$$V = 4\sqrt{6}\left[\frac{\pi}{2} - \arctan\left(y_1^{-1}\left(\sqrt{1 - X_1^2/3X_*^2} + \sqrt{2}X_1/\sqrt{3}X_*\right)\right)\right]X_* + X_1 d \quad (10)$$

for the case of $X_*/\sqrt{3} < X_1 < X_*$, and

$$V = (4\sqrt{2}/3)C_m^{3/2} X_*^3 I^{-2} + 2\sqrt{2C_m}(\sqrt{3}X_* - X_1)X_* I^{-1} + 4\sqrt{6}\left[\frac{\pi}{2} - \arctan\left(C_2 y_1/2 + X_1/\sqrt{3}X_* y_1\right)\right]X_* + X_1 d \quad (11)$$

for the small current case, $X_1 < X_*/\sqrt{3}$. Figure 3 illustrates the $V - I$ curve in the case of $d = 20$. We have $V \propto X_*^3 I^{-2}$ in the small I limit. The voltage difference V is rewritten as $V = V_{peak} + X_1 d$, where V_{peak} is owing to the deviation of the solitary solution form the constant one. For the trivial solution Eq.(4), the voltage difference is given by $V = X_1 d$.

The solitary structure is characterized by the peak value of the radial electric field $X(0)$ and the radial width Δ. The condition $F(X(0)) = 0$ determines the peak value, and the peak value of $\sqrt{F(X)}$ gives the steepest gradient $|dX/dx|$. The results in the small radial current limit, $X(0) \propto X_*^2 I^{-1}$ and $V \propto X_*^3 I^{-2}$, are shown to hold generally. In the small I limit, an approximate relation $F(X) \sim F(X_2) - IX$ holds for a large value of X. The maximum of the function F, $F(X_2)$, scales as X_*^2. The solution of the equation $F(X(0)) = 0$ is approximately given as $X(0) \simeq F(X_2) I^{-1} \sim X_*^2 I^{-1}$. The peak value of $\sqrt{F(X)}$ is evaluated as $\sqrt{F(X_2)} \sim X_*$. That is, the gradient is estimated as

$$|dX/dx| \sim X_*, \quad (12)$$

apart from numerical factors of the order unity. The layer thickness is given by $\Delta = (X(0) - X_1)/|X'|$. In this case, we have $\Delta \sim X_* / I$. We have an estimate $V_{peak} \simeq (X(0) - X_1)\Delta$, and obtain a dependence as $V_{peak} \simeq X_*^3 I^{-2}$ in the small I limit. In the case of $I \simeq I_*$, it is explicitly calculated as $V_{peak} = 12C^{-5/4}(I_* - I)^{1/4} + \cdots$.

The bifurcation is described by the voltage-current relation. The V-I curve is a multi-valued function as is shown in Fig.3. For a fixed value of current, two solutions of V are given. For a fixed value of V, one, or three solutions of I are available.

We next discuss about the stability of the solution. Writing $X = X_0 + \delta X$, where X_0 is the stationary solution, one obtains that the perturbed voltage $\delta V = \int \delta X$ for the fixed value of I satisfies the relation $\frac{\partial}{\partial \tau}\delta V = -\int_{-d/2}^{d/2} dx\,[d\{Xf(X)\}/dX]_{X_0}\delta X$. For the homogeneous solution Eq.(4), one has $\partial(\delta V)/\partial\tau = -[d\{Xf(X)\}dX]_{X_1}\delta V$. The coefficient of δV in the right hand side is negative, i.e., the solution is stable. For the nontrivial solution, Eq.(6), the solution could be unstable. If $\delta X(x)$ is chosen such that $\delta X(x) = 0$ holds in the region $X_0(x) < X_*$, the coefficient $C_V = -\int_{-d/2}^{d/2} dx \left[\frac{d}{dX}Xf(X)\right]_{X_0} \delta X \left(\int_{-d/2}^{d/2} dx\,\delta X\right)^{-1}$ is positive. The perturbed voltage satisfies the relation $d\delta V/dt = C_V \delta V$ and is unstable for a fixed current. In experimental condition, the external circuits are often composed of the power supply of V_{ext} and the internal resistance. Then the applied voltage between the electrode V and the current density I is constrained as $V = V_{ext} - \hat{r}_i I$ (coefficient $\hat{r}_i$ is proportional to the internal resistance), as is shown by the solid (or dashed) lines in Fig.3. The cross-points of the V-I curve and the constraints $V = V_{ext} - \hat{r}_i I$ give the solutions. In the cases of high and low V_{ext} (thin solid lines), solutions are given by A or C and are stable. Bifurcation from the constant one to the solitary structure takes place at A', and the back transition occurs at C'. When three roots are given (thin dashed-dotted line), the second solution B is unstable. We see a hysteresis of the electric field structure as a function of the voltage in the power supply. Depending on the characteristics of the external circuit, this system also shows the limit cycle oscillation. The details will be reported in a separate article.

Finally, the influence of the radial electric field inhomogeneity on the ion viscosity is investigated. The shear viscosity of ions has two origins, one is the collisional transport, μ_c, and the other is the turbulent transport, μ_N. The turbulent transport could depend on the electric field gradient, and the ratio $|\omega_{EI}/\gamma_{dec}|$ is the key parameter, where $\omega_{EI} = (dE_r/dr)B^{-1}$ and γ_{dec} is the nonlinear decorrelation rate of the fluctuations that cause the turbulent transport [5-7]. Analytic formulae have been derived as $\mu_N = \mu_N(0)(1 + \omega_{EI}^2/\gamma_{dec}^2)^{-1}$ (when $|\omega_{EI}/\gamma_{dec}|$ is small) and $\mu_N \propto \mu_N(0)|\omega_{EI}/\gamma_{dec}|^{-\nu}$ (when $|\omega_{EI}/\gamma_{dec}|$ is large, $\nu < 1$). We chose, as an interpolation formula, as

$$\mu_N = \mu_N(0)\left(1 + (2/\nu)\left(\omega_{EI}/\gamma_{dec}\right)^2\right)^{-\nu/2} . \tag{13}$$

The explicit form of the coefficient γ_{dec} is given in, e.g., [3]. Introducing normalized coefficients as, $H_1 \equiv \left(eT/\gamma_{dec}B\ell\rho_p\right)^2$, $\mu_{i0} \equiv \mu_i(X \to 0) = \mu_N(X \to 0) + \mu_c$, and $\eta \equiv \mu_N(X \to 0)/\mu_{i0}$, we rewrite as $\mu_i = \mu_{i0}\left\{1 - \eta + \eta\left(1 + (2/\nu)H_1(dX/dx)^2\right)^{-\nu/2}\right\}$. Length ℓ is defined as $\ell = \sqrt{\mu_{i0}/\sigma(0)}$. Equation (5) is replaced as

$$\frac{\eta\nu}{4H_1}\left\{\frac{1}{1-\nu/2} + \frac{1-\nu}{1-\nu/2}\left(1 + \frac{2H_1}{\nu}\left(\frac{dX}{dx}\right)^2\right)^{1-\nu/2} - 2\left(1 + \frac{2H_1}{\nu}\left(\frac{dX}{dx}\right)^2\right)^{-\nu/2}\right\}$$
$$+ \frac{1}{2}(1-\eta)\left(\frac{dX}{dx}\right)^2 = F(X) \tag{14}$$

Equation (14) provides a self-consistent solution for E_r and turbulence suppression. The peak value of X, $X(0)$, is not modified, because it is determined by the relation $F(X(0)) = 0$. The solution $|x| > \Delta$ has also the same asymptotic form. The coupling with the suppression of the turbulent transport makes the solitary structure of E_r more peaked, but does not change the qualitative nature. If the coefficient H_1 is small, $(2/\nu)H_1X_*^2 << 1$, the solution $X(x)$ is unaltered from Eq.(6), and the maximum suppression factor is given as $\mu_N/\mu_N(0) \simeq \left(1 + H_1X_*^2\right)^{-1}$. In an intermediate range, $1 << (2/\nu)H_1X_*^2 << \left((1-\nu)/(1-\nu/2)\right)^{2/\nu}\eta^{2/\nu}(1-\eta)^{1-2/\nu}$, the left hand side of Eq.(14) is approximated as $\eta\nu^{\nu/2}(1-\nu)(1-\nu/2)^{-1}H_1^{-\nu/2}2^{-1-\nu/2}(dX/dx)^{2-\nu}$. Equating it with

the maximum of F, the maximum of the gradient is estimated as $X' \simeq (X_*^2(1-\nu/2)/(1-\nu))^{1/(2-\nu)}(2H_1/\nu)^{\nu/(4-2\nu)}$ and the maximum suppression factor is given as $\mu_N/\mu_N(0) \simeq (2H_1X_*^2(1-\nu/2)/\nu(1-\nu))^{-\nu/(2-\nu)}$. In a case of large coefficient H_1, $((1-\nu)/(1-\nu/2))^{2/\nu}\eta^{2/\nu}(1-\eta)^{1-2/\nu} << (2/\nu)H_1X_*^2$, the left hand side of Eq.(14) is approximated as $2^{-1}(1-\eta)(dX/x)^2$: The maximum of the gradient is approximately given as $X' \simeq (1-\eta)^{-1/2}X_*$. The maximum suppression factor is given as $\mu_N/\mu_N(0) \simeq (1-\eta)^{-2/\nu}(2H_1X_*^2/\nu)^{-\nu/2}$, satisfying the relation $\mu_N < (1-\nu/2)(1-\nu)^{-1}\mu_c$. The anomalous transport coefficient is reduced to the level of collisional one and the momentum transport barrier is locally formed.

In summary, the solitary-ring structure of the radial electric field in the tokamak plasmas is obtained. The stable solitary structure is sustained by the external steady power supply. The radial gradient is governed by the ion viscosity and the nonlinearlity of the perpendicular conductivity. The radial structure and the suppression of the turbulent transport are self-consistently obtained. This solitary structure is a typical example of the structural formation associated with the electric field bifurcation and the reduction of the turbulent transport. The solution Eq.(6) includes the one in which multiple solitary structures are confined between the electrodes. Such solutions will be discussed in a separate article. In this article we neglected, for the analytic transparency, the neutral particle which causes a radial current $J_{r,n} = \sigma_n E_r$. The coefficient σ_n is proportional to the neutral particle density n_0 and is independent of E_r. If n_0 is so high that the condition $\sigma_n/\sigma(0) << I/X_{max} \sim I^2/X_*^2$ is not satisfied, the influence of neutral particles must be kept. Such a correction will be reported in a separate article.

Authors acknowledge discussion with Prof. R. R. Weynants. The work is partly supported by the Grant-in-Aid for Scientific Research of Ministry of Education, Science, Sports and Culture of Japan, by the collaboration programme of NIFS and by the collaboration programme of Advanced Fusion Research Center of Kyushu University.

References

[1] Wagner F *et al* 1982 *Phys. Rev. Lett.* **49** 1408.

[2] Itoh S-I, Itoh K 1988 *Phys. Rev. Lett.* **60** 2276.

[3] Itoh K and Itoh S-I 1996 *Plasma Phys. Contr. Fusion* **38** 1.

[4] Burrell K H 1997 *Phys. Plasmas* **4** 1499.

[5] Itoh S-I, Itoh K, Ohkawa T, Ueda N 1989 in *Plasma Physics and Controlled Nuclear Fusion Research 1988* (IAEA, Vienna) Vol.2, p23.

[6] Shaing K C *et al* 1989 in *Plasma Physics and Controlled Nuclear Fusion Research 1988* (IAEA, Vienna) Vol.2, p13.

Zhang Y Z, Mahajan S M 1992 *Phys. Fluids B* **4** 1385.

[7] Biglari H, Diamond P H, Terry P W 1990 *Phys. Fluids B* **2** 1.

[8] Hastings D E, Hazeltine R D, Morrison P J 1986 *Phys. Fluids* **29** 69.

[9] Itoh S-I, Itoh K, Fukuyama A, Miura Y 1991 *Phys. Rev. Lett.* **67** 2485.

[10] Weynants R R *et al* 1992 *Nucl. Fusion* **32** 837.

Taylor R J *et al* 1989 *Phys. Rev. Lett.* **63** 2365.

[11] Cornelis J, et al. 1994 *Nucl. Fusion* **34** 171.

Stringer T E 1993 *Nucl. Fusion* **33** 1249.

Figure Captions

Fig.1 Schematic drawing of the local current $f(X)X$ as a function of the electric field X. $f(X)X$ takes maximum I_* at $X = X_*$.

Fig.2 Solitary structure of the radial electric field. Model form $f(X)$ is taken as $f(X) = 1 - X^2/3X_*^2$ ($|X| < \sqrt{3}X_*$) and $f(X) = 0$ ($|X| > \sqrt{3}X_*$) Parameter is $X_I/X_* = 0.6$ ($I/I_* = 0.792$). Dotted line shows the trivial solution Eq.(4).

Fig.3 Relation between the voltage V and the current I for the solitary structure of E_r (thick solid line) and that of the constant solution of E_r (thick dashed line). (The distance is chosen as $d = 20$.) External circuit provides a constraint, $V = V_{ext} - \hat{r}_i I$, as is schematically shown by the thin lines. Bifurcation to the solitary structure takes place at A', and the back transition occurs at C'.

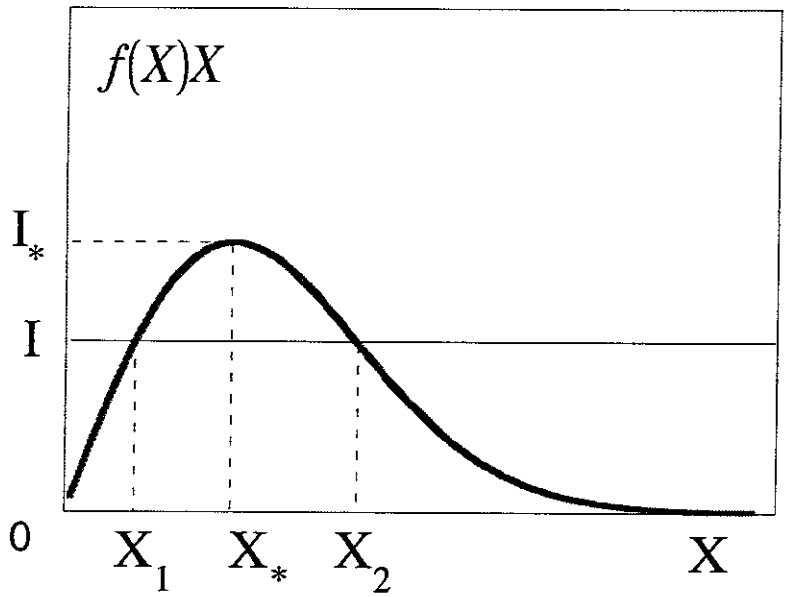

Fig.1

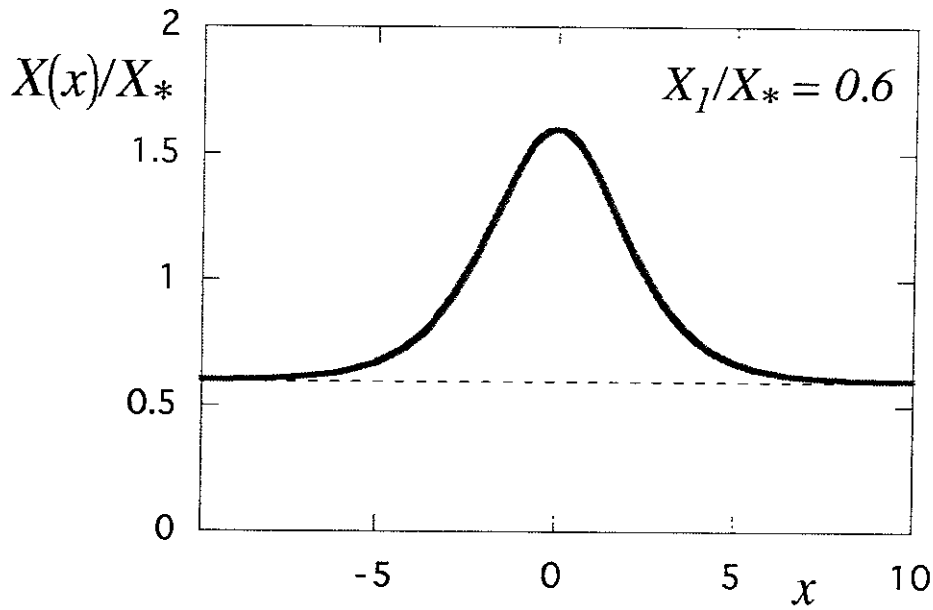

Fig.2

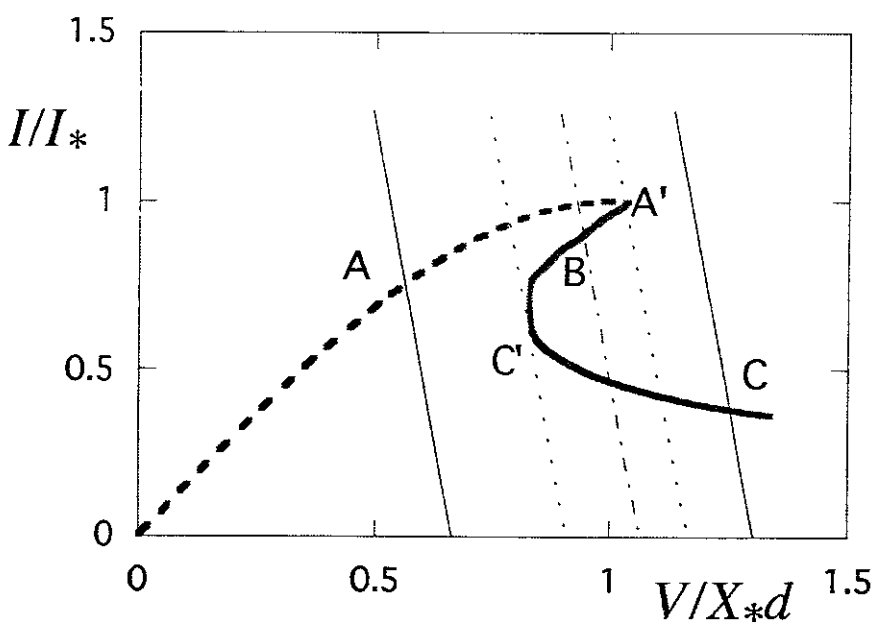

Fig.3

Recent Issues of NIFS Series

NIFS-477 H. Kuramoto, K. Toi, N. Haraki, K. Sato, J. Xu, A. Ejiri, K. Narihara, T. Seki. S. Ohdachi, K. Adati, R. Akiyama, Y. Hamada, S. Hirokura, K. Kawahata and M Kojima,
Study of Toroidal Current Penetration during Current Ramp in JIPP T-IIU with Fast Response Zeeman Polarimeter; Jan., 1997

NIFS-478 H. Sugama and W. Horton.
Neoclassical Electron and Ion Transport in Toroidally Rotating Plasmas; Jan. 1997

NIFS-479 V.L. Vdovin and I.V. Kamenskij,
3D Electromagnetic Theory of ICRF Multi Port Multi Loop Antenna; Jan. 1997

NIFS-480 W.X. Wang, M. Okamoto, N. Nakajima, S Murakami and N. Ohyabu,
Cooling Effect of Secondary Electrons in the High Temperature Divertor Operation; Feb. 1997

NIFS-481 K. Itoh, S.-I. Itoh, H. Soltwisch and H.R. Koslowski,
Generation of Toroidal Current Sheet at Sawtooth Crash; Feb. 1997

NIFS-482 K. Ichiguchi,
Collisionality Dependence of Mercier Stability in LHD Equilibria with Bootstrap Currents; Feb. 1997

NIFS-483 S. Fujiwara and T. Sato,
Molecular Dynamics Simulations of Structural Formation of a Single Polymer Chain: Bond-orientational Order and Conformational Defects; Feb. 1997

NIFS-484 T. Ohkawa.
Reduction of Turbulence by Sheared Toroidal Flow on a Flux Surface; Feb. 1997

NIFS-485 K. Narihara, K. Toi, Y. Hamada, K. Yamauchi, K. Adachi, I. Yamada, K. N. Sato, K. Kawahata. A. Nishizawa, S. Ohdachi, K. Sato, T. Seki, T. Watari, J. Xu, A. Ejiri, S. Hirokura, K. Ida, Y. Kawasumi, M. Kojima, H. Sakakita, T. Ido, K. Kitachi, J. Koog and H. Kuramoto.
Observation of Dusts by Laser Scattering Method in theJIPPT-IIU Tokamak Mar. 1997

NIFS-486 S. Bazdenkov, T. Sato and The Complexity Simulation Group,
Topological Transformations in Isolated Straight Magnetic Flux Tube; Mar. 1997

NIFS-487 M. Okamoto,
Configuration Studies of LHD Plasmas; Mar. 1997

NIFS-488 A. Fujisawa, H. Iguchi. H. Sanuki, K. Itoh, S. Lee, Y. Hamada. S. Kubo, H. Idei, R.

Akiyama, K. Tanaka, T. Minami, K. Ida, S. Nishimura, S. Morita, M. Kojima, S. Hidekuma, S.-I. Itoh, C. Takahashi, N. Inoue, H. Suzuki, S. Okamura and K. Matsuoka,
Dynamic Behavior of Potential in the Plasma Core of the CHS Heliotron/Torsatron; Apr. 1997

NIFS-489 T. Ohkawa,
Pfirsch - Schlüter Diffusion with Anisotropic and Nonuniform Superthermal Ion Pressure; Apr. 1997

NIFS-490 S. Ishiguro and The Complexity Simulation Group,
Formation of Wave-front Pattern Accompanied by Current-driven Electrostatic Ion-cyclotron Instabilities; Apr. 1997

NIFS-491 A. Ejiri, K. Shinohara and K. Kawahata,
An Algorithm to Remove Fringe Jumps and its Application to Microwave Reflectometry; Apr. 1997

NIFS-492 K. Ichiguchi, N. Nakajima, M. Okamoto,
Bootstrap Current in the Large Helical Device with Unbalanced Helical Coil Currents; Apr. 1997

NIFS-493 S. Ishiguro, T. Sato, H. Takamaru and The Complexity Simulation Group,
V-shaped dc Potential Structure Caused by Current-driven Electrostatic Ion-cyclotron Instability; May 1997

NIFS-494 K. Nishimura, R. Horiuchi, T. Sato,
Tilt Stabilization by Energetic Ions Crossing Magnetic Separatrix in Field-Reversed Configuration; June 1997

NIFS-495 T. -H. Watanabe and T. Sato,
Magnetohydrodynamic Approach to the Feedback Instability; July 1997

NIFS-496 K. Itoh, T. Ohkawa, S. -I.Itoh, M. Yagi and A. Fukuyama
Suppression of Plasma Turbulence by Asymmetric Superthermal Ions; July 1997

NIFS-497 T. Takahashi, Y. Tomita, H. Momota and Nikita V. Shabrov,
Collisionless Pitch Angle Scattering of Plasma Ions at the Edge Region of an FRC; July 1997

NIFS-498 M. Tanaka, A.Yu Grosberg, V.S. Pande and T. Tanaka,
Molecular Dynamics and Structure Organization in Strongly-Coupled Chain of Charged Particles; July 1997

NIFS-499 S. Goto and S. Kida,
Direct-interaction Approximation and Reynolds-number Reversed Expansion for a Dynamical System; July 1997

NIFS-500 K. Tsuzuki, N. Inoue, A. Sagara, N. Noda, O. Motojima, T. Mochizuki, T. Hino and T. Yamashina,

Dynamic Behavior of Hydrogen Atoms with a Boronized Wall; July 1997

NIFS-501 I. Viniar and S. Sudo,
Multibarrel Repetitive Injector with a Porous Pellet Formation Unit; July 1997

NIFS-502 V. Vdovin, T. Watari and A. Fukuyama,
An Option of ICRF Ion Heating Scenario in Large Helical Device; July 1997

NIFS-503 E. Segre and S. Kida,
Late States of Incompressible 2D Decaying Vorticity Fields; Aug. 1997

NIFS-504 S. Fujiwara and T. Sato,
Molecular Dynamics Simulation of Structural Formation of Short Polymer Chains; Aug. 1997

NIFS-505 S. Bazdenkov and T. Sato
Low-Dimensional Model of Resistive Interchange Convection in Magnetized Plasmas; Sep. 1997

NIFS-506 H. Kitauchi and S. Kida,
Intensification of Magnetic Field by Concentrate-and-Stretch of Magnetic Flux Lines; Sep. 1997

NIFS-507 R.L. Dewar,
Reduced form of MHD Lagrangian for Ballooning Modes; Sep. 1997

NIFS-508 Y.-N. Nejoh,
Dynamics of the Dust Charging on Electrostatic Waves in a Dusty Plasma with Trapped Electrons; Sep.1997

NIFS-509 E. Matsunaga, T.Yabe and M. Tajima,
Baroclinic Vortex Generation by a Comet Shoemaker-Levy 9 Impact; Sep. 1997

NIFS-510 C.C. Hegna and N. Nakajima,
On the Stability of Mercier and Ballooning Modes in Stellarator Configurations; Oct. 1997

NIFS-511 K. Orito and T. Hatori,
Rotation and Oscillation of Nonlinear Dipole Vortex in the Drift-Unstable Plasma; Oct. 1997

NIFS-512 J. Uramoto,
Clear Detection of Negative Pionlike Particles from H_2 Gas Discharge in Magnetic Field; Oct. 1997

NIFS-513 T. Shimozuma, M. Sato, Y. Takita, S. Ito, S. Kubo, H. Idei, K. Ohkubo, T. Watari, T.S. Chu, K. Felch, P. Cahalan and C.M. Loring, Jr,

The First Preliminary Experiments on an 84 GHz Gyrotron with a Single-Stage Depressed Collector; Oct. 1997

NIFS-514 T. Shjmozuma, S. Morimoto, M. Sato, Y. Takita, S. Ito, S. Kubo, H. Idei, K. Ohkubo and T. Watari,
A Forced Gas-Cooled Single-Disk Window Using Silicon Nitride Composite for High Power CW Millimeter Waves; Oct. 1997

NIFS-515 K. Akaishi,
On the Solution of the Outgassing Equation for the Pump-down of an Unbaked Vacuum System; Oct. 1997

NIFS-516 *Papers Presented at the 6th H-mode Workshop (Seeon, Germany)*; Oct. 1997

NIFS-517 John L. Johnson,
The Quest for Fusion Energy; Oct. 1997

NIFS-518 J. Chen, N. Nakajima and M. Okamoto,
Shift-and-Inverse Lanczos Algorithm for Ideal MHD Stability Analysis; Nov. 1997

NIFS-519 M. Yokoyama, N. Nakajima and M. Okamoto,
Nonlinear Incompressible Poloidal Viscosity in L=2 Heliotron and Quasi-Symmetric Stellarators; Nov. 1997

NIFS-520 S. Kida and H. Miura,
Identificaiton and Analysis of Vortical Structures; Nov. 1997

NIFS-521 K. Ida, S. Nishimura, T. Minami, K. Tanaka, S. Okamura, M. Osakabe, H. Idei, S. Kubo, C. Takahashi and K. Matsuoka,
High Ion Temperature Mode in CHS Heliotron/torsatron Plasmas; Nov. 1997

NIFS-522 M. Yokoyama, N. Nakajima and M. Okamoto,
Realization and Classification of Symmetric Stellarator Configurations through Plasma Boundary Modulations: Dec. 1997

NIFS-523 H. Kitauchi,
Topological Structure of Magnetic Flux Lines Generated by Thermal Convection in a Rotating Spherical Shell; Dec. 1997

NIFS-524 T. Ohkawa,
Tunneling Electron Trap; Dec. 1997

NIFS-525 K. Itoh, S.-I. Itoh, M. Yagi, A. Fukuyama,
Solitary Radial Electric Field Structure in Tokamak Plasmas; Dec. 1997